J Mater Sci: Mater Med (2012) 23:2553–2562
DOI 10.1007/s10856-012-4714-3

Assessment of in vitro temporal corrosion and cytotoxicity of AZ91D alloy

Costantino Del Gaudio · Paolo Bagalà · Marco Venturini · Claudio Grandi · Pier Paolo Parnigotto · Alessandra Bianco · Giampiero Montesperelli

Received: 30 June 2011 / Accepted: 26 June 2012 / Published online: 17 July 2012

Abstract Magnesium alloys represent a valuable option for the production of bioresorbable implantable medical devices aimed to improve the therapeutic approach and minimize the potential risks related to biostable materials. In this regard, the degradation process needs to be carefully evaluated in order to assess the effectiveness of the regenerative support and the eventual toxic effects induced by the released corrosion products. Aluminium is one of the most common alloying element that raised several safety concerns, contributing to shift the investigation toward Al-free alloys. To delve into this issue, a long-term investigation (up to 28 days) was performed using AZ91D alloy, due to its relevant Al content. Immersion tests in phosphate buffered saline (PBS) solution was performed following the ASTM standards and the corrosion behaviour was evaluated at fixed time points by means of electrochemical techniques. Cytotoxic effects were assessed by culturing human neuroblastoma cells with conditioned medium derived from immersion tests at different dilution degree. An increase in the resistance corrosion with the time was observed. In all the investigated cases the presence of Al in the conditioned media did not induce significant toxic effects directly correlated to its content. A decrease of cell viability was only observed in the case of 50 % dilution of PBS conditioned for the longest immersion period (i.e., 28 days).

C. Del Gaudio (✉) · P. Bagalà · A. Bianco · G. Montesperelli (✉)
Department of Industrial Engineering, INSTM Research Unit Tor Vergata, University of Rome "Tor Vergata", Via del Politecnico 1, 00133 Rome, Italy
e-mail: costantino.delgaudio@uniroma2.it

G. Montesperelli
e-mail: montesperelli@stc.uniroma2.it

M. Venturini · C. Grandi · P. P. Parnigotto
Department of Pharmaceutical Sciences, University of Padua, Via Marzolo 5, 35100 Padua, Italy

1 Introduction

The development of bioresorbable medical devices can be regarded as a potential improvement for the treatment of several pathologies, also having a positive effect on the outcome and the quality of life of recipients. The pivotal concept of this alternative therapeutic approach is to support tissue regeneration and healing by material degradation and concurrent implant replacement through the surrounding tissue. To date, the implant market is experiencing a huge demand, considering that approximately 2 million cases of artificial articulation replacement are registered worldwide and more than 1 million endovascular stents are implanted each year [1]. Therefore, the appropriate selection of a suitable bioresorbable material depends on several crucial requirements, e.g., biocompatibility, mechanical properties, degradation rate and absence of toxic by-degradation products. In particular, the latter topic represents a relevant issue to be addressed taking into account not only the eventual local adverse response following the surgical implantation, but also the systemic reaction in the mid- and long-term period.

Magnesium alloys are currently investigated as potential materials to be used for orthopaedic and endovascular treatments. It is known that the degradation takes place in aqueous environments via an electrochemical reaction which produces magnesium hydroxide and hydrogen. In water environment magnesium hydroxide accumulates on the underlying matrix as a corrosion protective layer, turning to a highly soluble magnesium chloride when the

chloride concentration in the corrosive environment rises above 30 mmol/L [2]. Reasonably, the alloy composition plays a relevant role in the definition of the degradation rate and the release of potentially toxic products. In this respect a great effort is pursued toward the analysis and the selection of the appropriate magnesium alloy to be safely implanted, considering that several alloying elements are investigated as potentially toxic. For instance, the presence of aluminium is generally regarded as a risk factor, being implicated in the onset of different degenerative pathologies, e.g., Alzheimer's disease (AD), muscle fiber damage, and decreased osteoclast viability, as resumed by Witte et al. [2]. Michalke et al. [3] reported that the linkage between aluminium and AD is controversially discussed, starting a debate whether aluminium is deposited in brain as a result of AD or whether it acts as its inducer or accelerator and concluding that is neurotoxic and cannot be disregarded as a factor in AD. On the other hand, it was also reported that a binary Mg–Al alloy did not show negative effects on the viability of blood vessel related cells, human umbilical vein endothelial cells and rodent vascular smooth muscle cells [4]. Moreover, open pore AZ91D scaffolds implanted in rabbits showed a good biocompatibility and reacted in vivo with an appropriate inflammatory host response [5].

The debated adverse effects contributed to shift the research toward the development of aluminium free magnesium alloys. Therefore, rare earth (RE) alloying elements are constantly gaining a particular attention for the definition of feasible magnesium-based medical devices. However, it should be underlined that this alternative option is not fully investigated and the mid- and long-term effects of RE elements need to be clarified. Several concerns on their biological role were previously highlighted, e.g., the incidence of RE on bone marrow cells need a detailed investigation because the clearance from the bone is known to be very slow [6]. It was also reported that ionic RE easily form colloid in blood and the resulting colloid material is taken by phagocytic cells of the liver and spleen [6]. Moreover, RE ions cause haemolysis at very low concentrations, in the range 3–17 $\times$ 10^{-7} M/L, by inducing domain and pore formation of the erythrocyte membrane [4]. It was also previously reported that (i) light RE elements are known to be hepatotoxic [7], (ii) Pr is the most toxic element leading to animal death in comparable concentrations used for Ce, probably due to the low clearing rate [7], and (iii) Pr and Nd induce chromosome aberrations in mice in vivo [8]. The investigation of RE metals used in magnesium-based vascular stents revealed no major adverse effects on the proliferation of smooth muscle cells when added as low concentrated alloying elements, while led to the upregulation of inflammatory genes at high concentrations [9]. Recently, Feyerabend et al. [10] evaluated the short-term effects of RE on primary cells and cell lines, reporting that La and Ce showed the highest cytotoxicity.

Therefore, due to the potential toxic effects of magnesium-alloying elements and in order to evaluate the response to an in vitro prolonged experimental protocol, the temporal corrosion of the AZ91D alloy was investigated by means of electrochemical techniques. The rationale of this study was to focus on the magnesium alloy that raises several concerns as a material for implantable devices, due to the presence of Al and its biological implications. The acquired data were correlated to the results of an indirect cytotoxic assay that can be considered a valuable approach to infer on the actual influence of the by-degradation products of magnesium alloy [4, 10–12]. Despite the usually reported linkage of Al to neural diseases as the primary cause that negatively affects the use of this element, several studies tested the compatibility of Mg alloy containing Al by using different cell lineages, e.g., fibroblast cells, human umbilical vein endothelial cells and rodent vascular smooth muscle cells, or bone-related cells [4, 11, 13]. Therefore, in order to complete this investigational topic a well established neural model needed to be considered, as the one here proposed, i.e., human neuroblastoma cells SH-SY5Y. In this overall context, the present analysis is expected to furnish further insights on the effects of this magnesium-alloying element for a long-term in vitro treatment.

2 Materials and methods

2.1 Material and sample preparation

AZ91D die casting magnesium alloy was used for this study (9.0 wt% Al; 0.7 wt% Zn; <0.13 wt% Mn; <0.1 wt% Si; <0.005 wt% Fe; <0.002 wt% Ni; <0.030 wt% Cu).

Three different sets of samples were prepared, for as many tests, according to ASTM G31 standard [14] that provides a solution-to-specimen area ratio of 0.40 mL/mm^2.

Weight loss measurements were carried out on cylindrical specimens, 20 mm in diameter and 2 mm in height. Samples were immersed in phosphate buffered saline (PBS) solution (Invitrogen S.r.l. Milan, Italy), and incubated at 37 °C, 95 % relative humidity and 5 % CO_2. After 7, 14 and 28 days, samples were withdrawn from the solution, dried in air at room temperature and the corrosion products were removed according to ASTM G1 standard [15]. The etching solution consisted in 200 g chromium trioxide (CrO_3), 10 g silver nitrate ($AgNO_3$) and 20 g barium nitrate ($Ba(NO_3)_2$) for 1 L deionized water. After the determination of weight losses, samples were observed by scanning electron microscopy (SEM) and analyzed by energy dispersive spectroscopy (EDS). The solutions were

analyzed by inductively coupled plasma mass spectrometry (ICP-MS) (Agilent Technologies 7500C).

PBS solutions, in which AZ91D bar specimens were incubated, were used to evaluate cytotoxicity by means of MTS assays (described in the following).

Finally, cylindrical specimens (diameter = 20 mm, exposed area = 3.14 cm^2), mounted in epoxy resin and electrically connected by an electrical wire, were used for electrochemical tests. The samples were grinded with 1,200 grit SiC abrasive paper and then polished with 3 μm diamond paste and tested immediately.

2.2 Microstructural characterization

Sample microstructure before and after immersion tests was observed by means of SEM (LEO Supra 35), equipped with EDS (INCA Energy 300, detector Oxford ELXII). Quantitative analyses were performed by means of a calibration line recorded on a pure cobalt reference standard in a wide range of counts per second. For each analyzed element a reference standard was performed using a pure sample.

Sample microstructure before immersion was evaluated after chemical etching with a picric acid solution (5 g picric acid, 100 mL ETOH and 10 mL H_2O).

Phase analysis was performed by means of X-ray diffraction (XRD, Philips X'Pert 1710, Cu-Kα radiation $\lambda = 1.54056$ Å, 10–80° 2θ, step size 0.020°, time per step 2 s, scan speed 0.005°/s).

2.3 Electrochemical measurements

Electrochemical impedance spectroscopy (EIS) measurements were carried out with a Solartron 1287 electrochemical interface and a Solartron 1260 frequency response analyser (FRA) at room temperature in PBS solution. An alternating signal, 5 mV in amplitude, was applied at the open circuit potential (OCP) in the frequency range from 10^{-2} to 10^5 Hz. A platinum plate and a Ag/AgCl electrode were used as counter and reference electrode, respectively. EIS measurements were performed on mounted samples immersed in PBS incubated for 7, 14, 28 days. EIS spectra were acquired by Zplot and evaluated by Zview softwares (Scribner Associates), using non linear least squares (NLLS) method (test χ^2). Blank tests were also performed.

The polarization curves were acquired on the same samples 30 min after EIS tests. The scan rate used was 1.67 mV/s. The corrosion current was extrapolated by the Tafel slopes.

2.4 Cell culture

SH-SY5Y cells, derived from human neuroblastoma, were purchased from the European Animal Cell Culture Collection (EACC, Porton Down, Wilts, UK) and cultured in Dulbecco's Modified Eagles Medium: Nutrient Mixture F-12 (DMEM/F-12) (Invitrogen Life Technology, Carlsbad CA) with 15 % Fetal Bovine Serum (FBS), Penicillin (100 mg/ml), Streptomycin (100 mg/ml), 1 % Non Essential Aminoacid (NEAA) (Sigma-Aldrich, St. Louis, MO) in standard incubator conditions (37 °C, 95 % relative humidity, 5 % CO_2).

2.5 MTS assay

To determine the effects of Mg alloy AZ91D on SH-SY5Y viability, cell redox activity was monitored by the colorimetric MTS assay (3-(4,5-dimethylthiazol-2-yl)-5-(3-carboxymethoxyphenyl)-2-(4-sulfophenyl)-2H-tetrazolium, inner salt) (CellTiter 96 Aqueous Assay, Promega, Madison, Wisconsin). Metabolically active cells react with a tetrazolium salt in the MTS reagent to produce a soluble formazan dye that can be observed at wavelength of 490 nm. SH-SY5Y cells were seeded (5×10^4 cells/cm^2) on a 96-well tissue culture-treated plates (Falcon BD Biosciences, San Jose, CA) and cultured in standard conditions. After 24 h from seeding, cells were treated with serum free medium containing 10, 30, 50 % PBS and medium containing 10, 30, 50 % PBS previously incubated with AZ91D alloy for 7, 14, 28 days. After 2, 4, 7 days of treatment, medium was replaced with a fresh one containing 20 % MTS reagent for 90 min. Aliquots were then transferred into 96 well plates and the absorbance at 490 nm read with Ultra Microplate Reader (Bio-Tek Instruments, Winooski, Vermont).

Statistical comparison was performed by the analysis of variance, followed by Student's t test.

2.6 Cellular morphology analysis

Optical morphology was evaluated by toluidine blue (Sigma-Aldrich, St. Louis, MO) staining on SH-SY5Y cells seeded on an optical cover glass in 24-well tissue culture-treated plates (Falcon BD Biosciences, San Jose, CA), at the same density of cytotoxicity test. After 24 h from seeding, cells were treated with serum free medium containing 10, 30, 50 % PBS and medium containing 10, 30, 50 % PBS previously incubated with AZ91D alloy for 7, 14, 28 days. At the end of incubation time, cells were washed in PBS and fixed in 3.7 % formalin solution at 4 °C, washed again with PBS and then stained with fresh toluidine solution (0.5 % w/v) for 10 s. After three water washes, optical cover glass were mounted on microscope holder glass with Eukitt (Sigma-Aldrich, St. Louis, MO) mounting medium. Cell morphology was observed by optical microscopy (Leica DM/IL; Leica Microsystems, Mannheim, Germany).

3 Results and discussion

3.1 Structural characterization

The optical metallography of the AZ91D alloy before test is shown in Fig. 1. The microstructure is characterized by the presence of large grains (about 200 μm in diameter) of a main constituent and precipitates of a second phase. EDS analysis (summarized in Table 1) confirmed that the major phase is mainly composed of Mg, while the second phase presented a higher Al and Zn content with respect to the primary phase. The XRD diffraction pattern (Fig. 2) showed the reflections associated to the presence of the two phases characteristic of the AZ91D alloy, i.e., Mg solid solution as main phase and the intermetallic compound $Mg_{17}Al_{12}$ as second phase.

SEM observation of AZ91D specimens after 7, 14 and 28 days of soaking in PBS solution demonstrated that the corrosion products tend to settle onto the surface of the Mg alloy, forming a thick layer (Fig. 3a). Most probably, the presence of deep cracks within the film is due, to the shrinkage occurring during the drying process. Chemical etched samples, instead, indicated that the alloy was affected by uniform corrosion. As an example, Fig. 3 reports SEM micrographs of AZ91D alloy after 7 days of soaking in PBS before (Fig. 3a) and after chemical etching (Fig. 3b). Moreover, EDS analysis revealed, as expected, an increased Al and Zn content as a consequence of the strong loss of Mg with immersion time (Table 1).

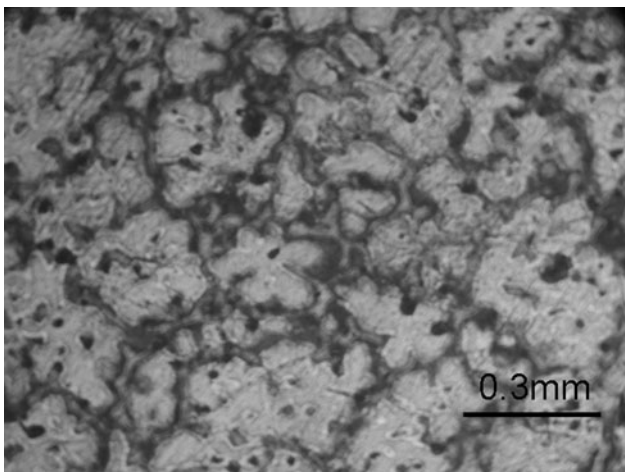

Fig. 1 Optical metallography of AZ91D alloy

Table 1 Energy dispersive spectroscopy of AZ91D samples

Sample	Mg (at.%)	Al (at.%)	Zn (at.%)	Al/Mg
As-received (main phase)	91.7	7.8	0.5	0.09
As-received (second phase)	61.7	32.8	2.2	0.53
7 days	79.9	19.3	0.9	0.24
14 days	71.8	26.7	1.5	0.37
28 days	58.8	38.8	2.3	0.66

The results of the weight loss tests are reported in Table 2, in which the weight loss (**Δ**w) in mg, the exposed area (A) in dm^2, the weight loss rate (v_w) in mdd and the corrosion rate (v_c) in mm/y are reported for each sample. As expected, v_w and v_c decreased with the immersion time. After 28 days in PBS they halved with respect to the values measured at 7 days due to the formation of a partially protective film grown onto sample surface.

Results of ICP-MS are summarized in Table 3. Mg concentration increased during the experimental period due to the ongoing degradation process while a remarkable decreasing trend has been observed for Al, most probably associated to the precipitation of aluminium hydroxide-based compounds in solutions of progressively increased pH (see below). Zn concentration was always lower than 0.1 μg/L and the amount of Mn slightly increased at 28 days compared to the previous time points.

3.2 Electrochemical measurements

Figure 4 shows the impedance spectra in the Nyquist representation, acquired after 0, 7, 14 and 28 days of immersion in PBS. As a general trend, a strong increase in the total resistance with immersion time can be detected as a result of the film formation. Data were analyzed with the equivalent circuit procedure. Figure 5 represents the equivalent circuit used to fit impedance data, with R_{el} being the solution resistance, R_{ct} the charge transfer resistance, C_{dl} the double-layer capacitance, R_{pore} the pore resistance that is due to the formation of ionically conducting path across the film and C_{film} the capacitance of the film [16]. Constant phase elements (CPE) have been used instead of a real capacitance. The CPE parameters were converted into capacitance values following the reported procedure [17].

The EIS spectrum acquired at the immersion days clearly showed two semi-circles that may be attributed to charge transfer reaction and to the formation of a film on the electrode surface. This behavior may be unexpected since the sample was polished just before testing, anyway it is probably due to the extreme reactivity of the alloy that quickly formed a layer of Mg hydroxide on the surface [18].

As an example, Fig. 6 shows the fitting of experimental data using the equivalent circuit of Fig. 5. A perfect agreement between experimental and calculated data was obtained as evidenced by χ^2 test that gave values lower than 10^{-4}.

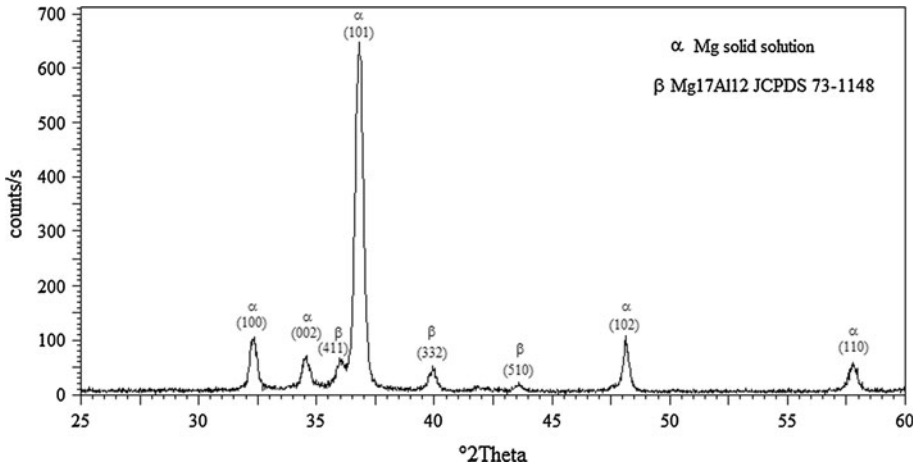

Fig. 2 XRD pattern of the AZ91D alloy

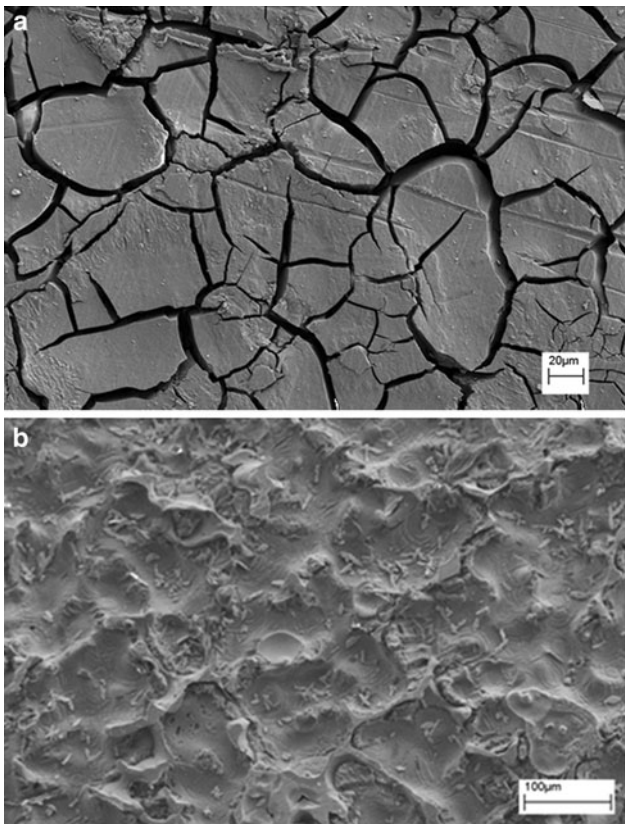

Fig. 3 Surface SEM micrographs of AZ91D alloy after 7 days of soaking in PBS before (**a**) and after chemical etching (**b**)

The semicircle related to the RC characteristics of the Faradaic reaction, cannot be detected in EIS spectra at 7, 14 and 28 days, due to its shift towards low frequency (clearly detectable in the Bode representation in Fig. 7) and to the large increase of film contribution.

Table 4 summarized the resistances values extrapolated by fitting the equivalent circuits. The R_{ct} value is reported only for samples at $t = 0$, since otherwise is negligible. The corrosion resistance raises with the immersion time. After 28 days of immersion the resistance is three times higher than the resistance at time zero. A similar behaviour was measured in the case of AZ31 samples immersed in PBS, phosphate ions can capture OH^- produced by the cathodic reaction and the alkaline pH that favours the massive precipitation of Mg hydroxide cannot be attained, but, on the other hand, the phosphate precipitation hinders the action of chloride, and Mg dissolution is slower [19, 20]. It is worth pointing out that a perfect agreement between EIS data and weight losses can be observed.

Figure 8 reports the polarization curves acquired in the same condition of EIS measurements. The analysis of polarization curves evidenced an active behaviour for all samples with a decrease of the corrosion current with time. Moreover, a significant ennoblement of the OCP with immersion time can be observed. The anodic curve for the AZ91D reference sample ($t = 0$) exhibited a knee point separating a slow (before) and a fast (after) increase of the current density. This behaviour indicated the formation of a partially protective surface film, mainly constituted of $Mg(OH)_2$, that cannot be considered a stable passive state due to the elevated values measured for the anodic current density [21]. The treated AZ91D samples at 7, 14 and 28 days did not clearly show this behaviour, since the growth of the magnesium phosphate layer heavily influenced the anodic process as confirmed by the values of Tafel slopes (b_a) reported in Table 4. As previously reported, magnesium phosphates and $Mg(OH)_2$ are the main corrosion products when PBS is used, insoluble carbonates can be also found possibly formed by the dissolved CO_2 in the solution [22].

It should be noted that the corrosion behaviour is strongly affected by the composition of the electrolyte solution, that limits the comparison among different experimentations and, mostly, prevents a direct correlation to the in vivo response. Xin et al. [23] investigated the degradation behaviour of AZ91 alloy in five different

Table 2 Weight loss of AZ91D samples

Immersion time (days)	Δw (mg)	A (dm^2)	$v_w = \|\Delta w\|/(A \cdot t)$ (mdd)	$v_s = v_w/\rho^a$ (mm/y)
7	26.2 ± 0.2	0.0634 ± 0.0001	59.0 ± 0.5	1.19 ± 0.01
14	51.2 ± 0.2	0.0644 ± 0.0001	56.8 ± 0.3	1.145 ± 0.006
28	50.0 ± 0.2	0.0641 ± 0.0001	27.9 ± 0.2	0.563 ± 0.004

[a] $\rho = 1.81$ g/cm^3 at T = 20 °C

Weight loss (**Δ**w), exposed area (A), weight loss rate (v_w), corrosion rate (v_c)

Table 3 Inductively coupled plasma mass spectrometry of AZ91D conditioned PBS

Sample (days)	Mg (mg/L)	Al (μg/L)	Zn (μg/L)	Mn (μg/L)
7	107.7 ± 0.6	4.9 ± 0.3	<0.1	3.2 ± 0.2
14	149.3 ± 1.3	1.0 ± 0.1	<0.1	3.1 ± 0.1
28	180.3 ± 2.2	0.4 ± 0.1	<0.1	3.8 ± 0.1

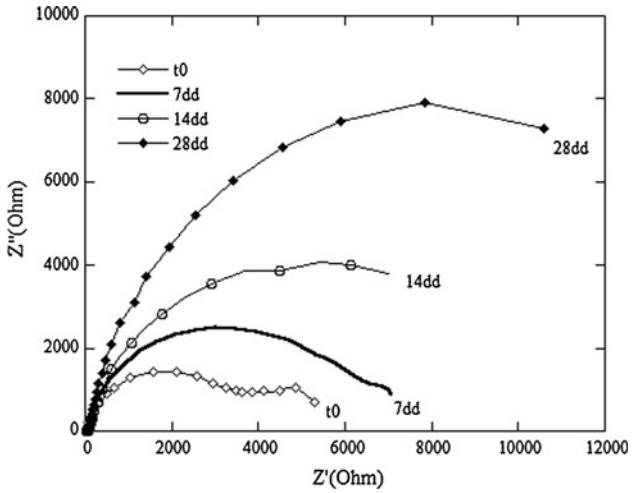

Fig. 4 Nyquist representation of EIS data as a function of immersion time

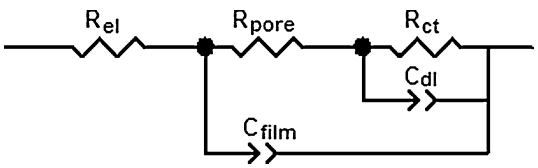

Fig. 5 Equivalent circuit used for EIS data fitting. R_{el} solution resistance, R_{ct} charge transfer resistance, R_{pore} pore resistance that is due to the formation of ionically conducting path across the film, C_{dl} double-layer capacitance, C_{film} capacitance of the film

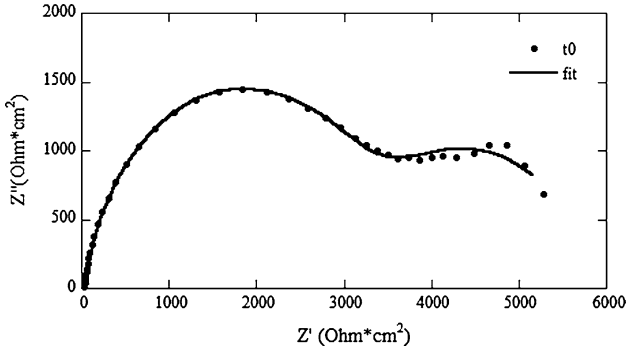

Fig. 6 Comparison between EIS data and curve fitting of the AZ91D blank sample in PBS solution

solutions: 0.9 % NaCl, PBS, simulated body fluid (SBF), Hank's solution and DMEM, being the typical solutions used for this kind of studies. They concluded that degradation measurements in Hank's solution is not convinced, since the concentration of bicarbonates is much lower compared to that in the plasma; SBF possesses a similar buffering capability as body fluids, but the concentration of bicarbonates depends on the type of selected SBF; finally, even if characterized by a higher buffering capability related to the HEPES amount, DMEM with similar ingredients and buffering capability as body fluids can be a suitable choice. However, also this latter vehicle can be affected by technical limitations as specified by ISO 10993-5 [24], in which is reported that cell culture medium should only be used in the extraction condition 24 ± 2 h at 37 ± 1 °C. At the same time, the above standard allows to select one or more suitable extraction vehicles for mammalian cells. Therefore, due to the large variability of test solutions, this study was aimed to assess the long-term degradation behaviour of AZ91D alloy (28 days) in a controlled in vitro set-up using a standard solution, i.e., PBS. In vitro tests can be suitable to study the corrosion of metal alloys as potential biomaterials, as stated by Mueller et al. [25] who used PBS to investigate the corrosion behaviour of pure Mg, AZ31 and LAE442.

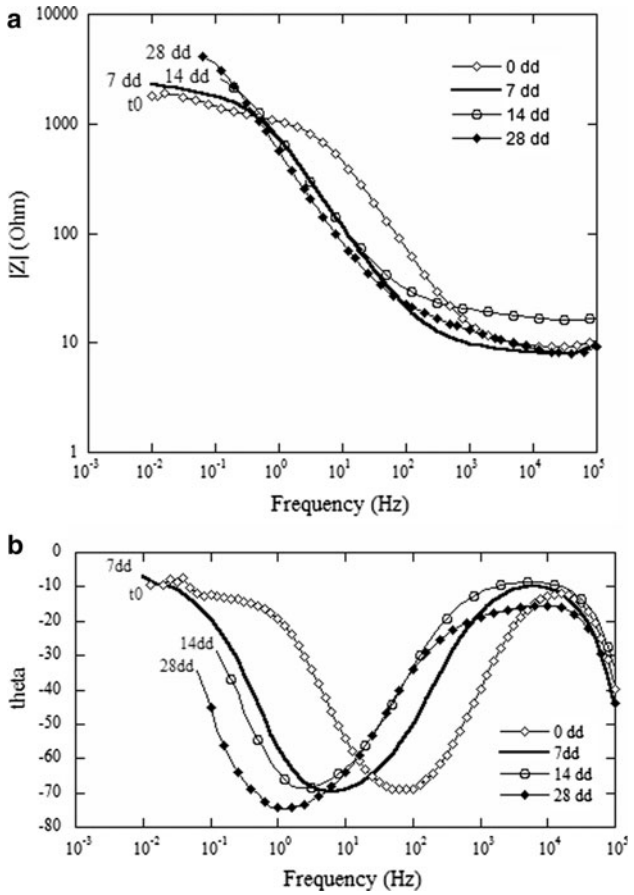

Fig. 7 Bode representation of EIS data as a function of immersion time, magnitude plot (**a**) and phase plot (**b**)

Table 4 Results of electrochemical measurements performed on AZ91D samples

Immersion time (days)	b_a (mV)	b_c (mV)	I_c ($\mu A/cm^2$)	E_c (V vs AgCl)	R (Ω)
0	203.71	161.19	8.97	−1.61	5819[a]
7	299.79	161.25	5.78	−1.57	7398
14	154.91	130.02	3.11	−1.52	9846
28	112.26	141.38	1.68	−1.52	20034

[a] $R_{ct} = 2303\ \Omega$; $R_{po} = 3516\ \Omega$. The charge transfer resistance (R_{ct}) and the pore resistance (R_{po}) were evaluated by EIS data fitting considering the equivalent circuit shown in Fig. 5

Anodic Tafel slope (b_a), catodic Tafel slope (b_c), corrosion current (I_c), corrosion potential (E_c), corrosion resistance (R)

3.3 Viability assay

SH-SY5Y cells were exposed to culture medium containing different percentage (10, 30, 50 %) of PBS previously incubated with the AZ91D alloy and its effect on cell viability was evaluated by MTS assay (Fig. 9). Figure 10 shows the morphology of SH-SY5Y cells cultured in

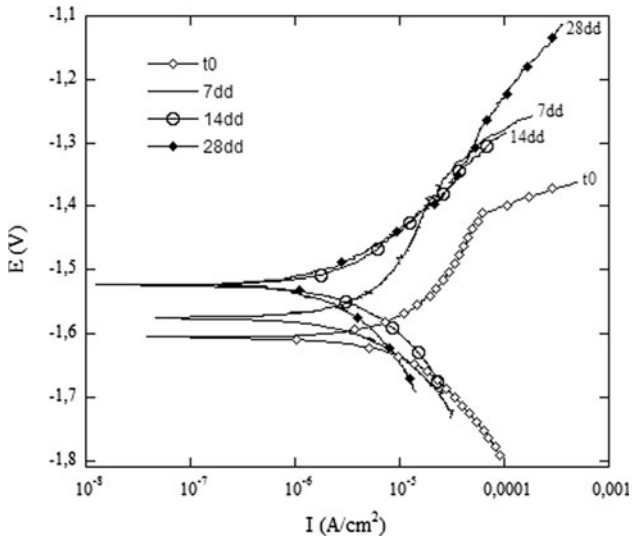

Fig. 8 Polarization curves for the AZ91D alloy before and after immersion in PBS for 7, 14, 28 days

28 days extracts at different concentration after 7 days incubation. It can be seen that the cells treated with the Mg alloy extracts in different dilutions were normal, similar to that of the control cultured in untreated culture medium. In order to emphasize the potential impact of the tested Mg alloy on the cytotoxicity, the medium was not changed throughout the cell incubation period. A significant ($p < 0.05$) cytotoxic effect was revealed after 4 and 7 days of treatment only for cells exposed to PBS solution incubated with AZ91D alloy for 28 days and only at the 50 % of dilution. At first, the reason for this behaviour might be ascribed to the Al presence in the culture medium, due to its high content as alloying elements and the toxic-related effects. In order to verify this hypothesis ICP-MS was performed to detect the Al concentration in the AZ91D conditioned PBS samples (Table 3). Referring to the here measured values, it should be considered that dietary intake of Al can vary from 3 to 30 mg/day and a definite relation was observed between urinary Al concentrations of 135 μg/L and cognitive performance [26]. Moreover, Michalke et al. [3] reviewed Al base values in serum being 5.4 μg/L as compared to 17 μg/L for AD patients, whereas in cerebrospinal fluid these values raised to 40 μg/L for young AD patients and 156 μg/L for old AD patients. Based on these observations and considering the PBS dilutions of the cell culture medium, a direct relationship between Al concentration and the decrease of cell viability does not seem straightforward.

At the same time, the pH of the solutions was also monitored, showing an increasing trend in AZ91D conditioned PBS from 7.53 (7 days) to 8.47 (28 days). As well known, the magnesium dissolution released OH^- that contributed to raise the pH of the cell culture medium.

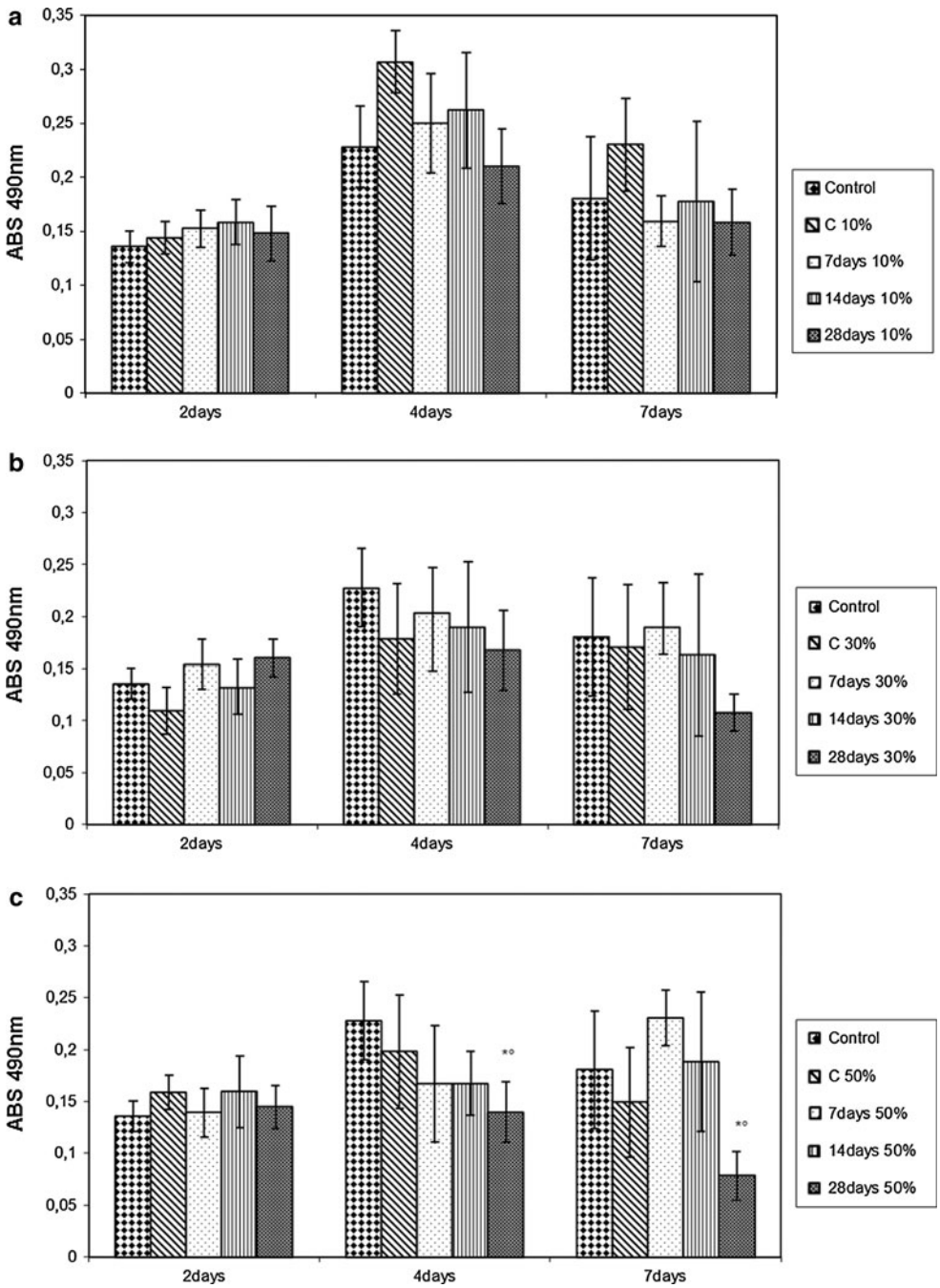

Fig. 9 MTS assay on SH-SY5Y cells after 2, 4 and 7 days of treatment with different concentration of 10 % (**a**), 30 % (**b**), 50 % (**c**) of PBS in culture medium. Control is the sample treated with culture medium. C10 %, C30 %, C50 % are the samples incubated with culture medium diluted at 10, 30, 50 % with sterile PBS. 7 days_%, 14 days_%, 28 days_% are the samples incubated with culture medium diluted at 10, 30, 50 % with PBS conditioned with AZ91D for 7, 14, 28 days (*$p < 0.05$ vs control, °$p < 0.05$ vs C50 %)

Cells are very sensitive to such environmental fluctuations and a considerable increment in the pH value negatively affect their viability [27]. The incidence of pH was previously reported for macrophages [13] cultured on AZ91D and human bone marrow-derived stromal cells exposed to AZ91D extracts, measuring a concentration of 0.52 ± 0.02 mg/L for Al released in DMEM [11]. Seuss et al. [28] focused on the role of corrosion-induced pH changes and confirmed that HeLa cell death increased with increasing alkalinity in the cell culture medium, also showing that cells attached on the AZ91D surface acted as corrosion-blocking layer that contributed to slow down the pH increase.

A technical issue was also critically considered in the discussion of the here presented results, being related to possible interference substances that could alter viability tests. Fischer et al. [29] investigated the effect of Mg corrosion on tretrazolium-based assays, showing its influence for the extract concentrations investigated (20–60 mM) and for high pH values (i.e., >9). These two conditions did not

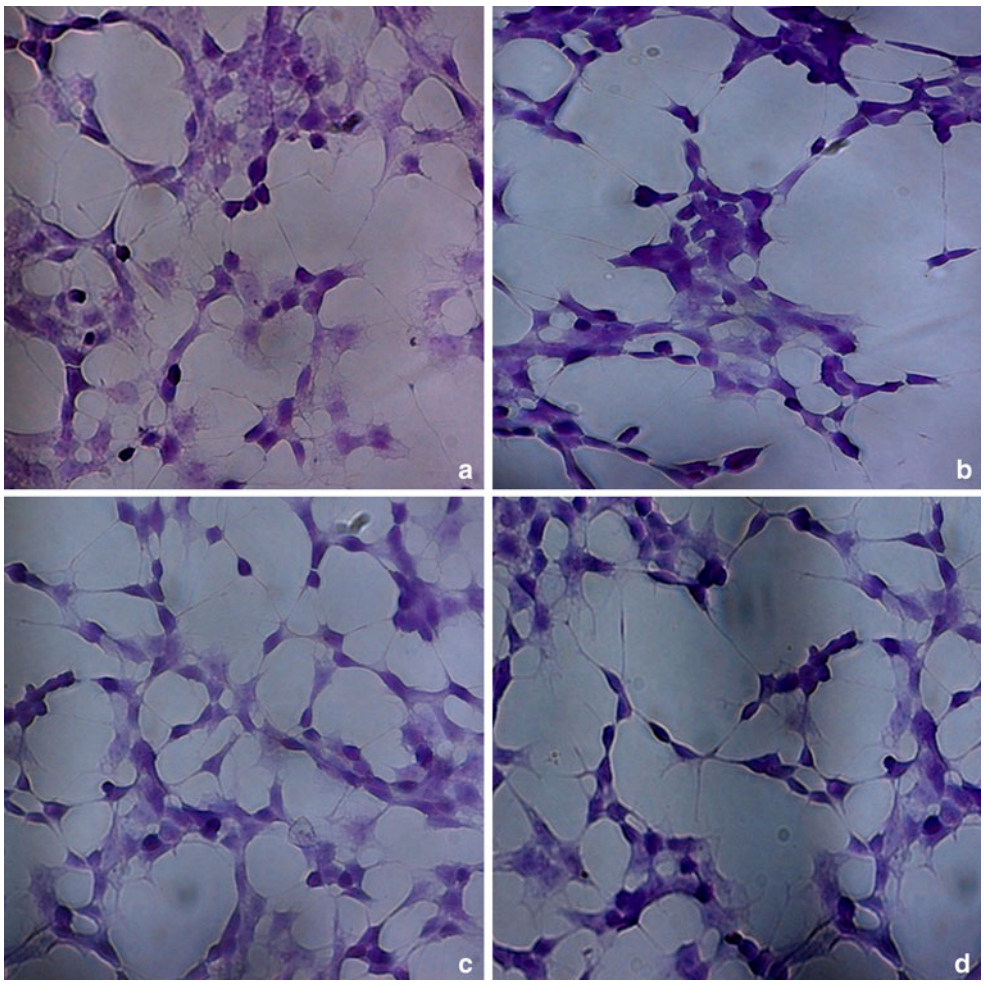

Fig. 10 Morphology of toluidine blue stained SH-SY5Y cells treated for 7 days with culture medium (**a**), culture medium diluted at 10 % (**b**), 30 % (**c**), and 50 % (**d**) with PBS conditioned with AZ91D for 28 days

occur in this experimental protocol as Mg concentration and pH value were lower than the reported levels in all the PBS solutions. On this basis, the incidence of the acquired findings was further enhanced.

Finally, the absence of significant differences between treated and control cases was verified for the 10 and 30 % solutions during the culture period, regardless of the temporal extent of AZ91D immersion in PBS.

4 Conclusions

Long-term immersion test induced the formation of a magnesium phosphate layer on the surface of AZ91D alloy that contributed to increase the corrosion resistance and decrease the corrosion current as measured by electrochemical tests. The potential toxic effects related to the Al content were indirectly investigated by means of MTS test that proved its reliability, as confirmed by ICP-MS analysis. Viability assay did not shown significant toxic effects for SH-SY5Y cells exposed to PBS solution at different dilution concentrations, except for the 50 % case after 28 days of AZ91D immersion. However, considering the concentrations of Al measured in this experimentation, this result cannot be directly related to the presence of released Al. The increased pH value in the saline solution can be reasonably implied in the observed cell behaviour.

References

1. Zeng R, Dietzel W, Witte F, Hort N, Blawert C. Progress and challenge for magnesium alloys as biomaterials. Adv Eng Mater. 2008;10:B3–14.
2. Witte F, Hort N, Vogt C, Cohen S, Kainer KU, Willumeit R, Feyerabend F. Degradable biomaterials based on magnesium corrosion. Curr Opin Solid State Mater Sci. 2008;12:63–72.

3. Michalke B, Halbach S, Nischwitz V. JEM spotlight: metal speciation related to neurotoxicity in humans. J Environ Monit. 2009;11:939–54.
4. Gu X, Zheng Y, Cheng Y, Zhong S, Xi T. In vitro corrosion and biocompatibility of binary magnesium alloys. Biomaterials. 2009;30(4):484–98.
5. Witte F, Ulrich H, Rudert M, Willbold E. Biodegradable magnesium scaffolds: Part I: appropriate inflammatory response. J Biomed Mater Res A. 2007;81:748–56.
6. Hirano S, Suzuki KT. Exposure, metabolism, and toxicity of rare earths and related compounds. Environ Health Perspect. 1996; 104(Suppl 1):85–95.
7. Nakamura Y, Tsumura Y, Tonogai Y, Shibata T, Ito Y. Differences in behaviour among the chlorides of seven rare earth elements administered intravenously to rats. Fundam Appl Toxicol. 1997;37(2):106–16.
8. Jha AM, Singh AC. Clastogenicity of lanthanides: induction of chromosomal aberration in bone marrow cells of mice in vivo. Mutat Res. 1995;341(3):193–7.
9. Drynda A, Deinet N, Braun N, Peuster M. Rare earth metals used in biodegradable magnesium-based stents do not interfere with proliferation of smooth muscle cells but do induce the upregulation of inflammatory genes. J Biomed Mater Res A. 2009;91(2): 360–9.
10. Feyerabend F, Fischer J, Holtz J, Witte F, Willumeit R, Drücker H, Vogt C, Hort N. Evaluation of short-term effects of rare earth and other elements used in magnesium alloys on primary cells and cell lines. Acta Biomater. 2010;6(5):1834–42.
11. Yang C, Yuan G, Zhang J, Tang Z, Zhang X, Dai K. Effects of magnesium alloys extracts on adult human bone marrow-derived stromal cell viability and osteogenic differentiation. Biomed Mater. 2010;5(4):045005.
12. Huan ZG, Leeflang MA, Zhou J, Fratila-Apachitei LE, Duszczyk J. In vitro degradation behavior and cytocompatibility of Mg–Zn–Zr alloys. J Mater Sci Mater Med. 2010;21(9):2623–35.
13. Witte F, Feyerabend F, Maier P, Fischer J, Störmer M, Blawert C, Dietzel W, Hort N. Biodegradable magnesium-hydroxyapatite metal matrix composites. Biomaterials. 2007;28(13):2163–74.
14. ASTM G31-72. Standard practice for laboratory immersion corrosion testing of metals. 2004.
15. ASTM G1-90. Standard practice for preparing, cleaning, and evaluating corrosion test specimens. 1999.
16. Mansfeld FB, Tsai CH. Determination of coating deterioration with EIS. Corrosion. 1991;47(12):958–63.
17. Hsu CS, Mansfeld F. Concerning the conversion of the constant phase element parameter Y_o into a capacitance. Corrosion. 2001; 57:747–8.
18. ASM metal handbook 9 Edition, ASM International Metals Park Ohio, vol 13, 1990. p. 742.
19. Alvarez-Lopez M, Pereda MD, del Valle JA, Fernandez-Lorenzo M, Garcia-Alonso MC, Ruano OA, Escudero ML. Corrosion behaviour of AZ31 magnesium alloy with different grain sizes in simulated biological fluids. Acta Biomater. 2010;6(5):1763–71.
20. Yang L, Zhang E. Biocorrosion behavior of magnesium alloy in different simulated fluids for biomedical application. Mater Sci Eng C. 2009;29(5):1691–6.
21. Rosalbino F, De Negri S, Saccone A, Angelini E, Delfino S. Biocorrosion characterization of Mg–Zn–X (X = Ca, Mn, Si) alloys for biomedical applications. J Mater Sci Mater Med. 2010;21(4): 1091–8.
22. Xin Y, Hu T, Chu PK. In vitro studies of biomedical magnesium alloys in a simulated physiological environment: a review. Acta Biomater. 2011;7(4):1452–9.
23. Xin Y, Hu T, Chu PK. Influence of test solutions on in vitro studies of biomedical magnesium alloys. J Electrochem Soc. 2010;157(7):C238–43.
24. Biological evaluation of medical devices - Part 5: Tests for in vitro cytotoxicity. ISO. 2009;10993–5.
25. Mueller WD, de Mele MF, Nascimento ML, Zeddies M. Degradation of magnesium and its alloys: dependence on the composition of the synthetic biological media. J Biomed Mater Res A. 2009;90(2):487–95.
26. Bharathi P, Vasudevaraju P, Govindaraju M, Palanisamy AP, Sambamurti K, Rao KS. Molecular toxicity of aluminium in relation to neurodegeneration. Indian J Med Res. 2008;128(4): 545–56.
27. Xin Y, Jiang J, Huo K, Tang G, Tian X, Chu PK. Corrosion resistance and cytocompatibility of biodegradable surgical magnesium alloy coated with hydrogenated amorphous silicon. J Biomed Mater Res A. 2009;89(3):717–26.
28. Seuss F, Seuss S, Turhan MC, Fabry B, Virtanen S. Corrosion of Mg alloy AZ91D in the presence of living cells. J Biomed Mater Res B Appl Biomater. 2011;99(2):276–81.
29. Fischer J, Prosenc MH, Wolff M, Hort N, Willumeit R, Feyerabend F. Interference of magnesium corrosion with tetrazolium-based cytotoxicity assays. Acta Biomater. 2010;6:1813–23.